第 34 卷 第 3 期
2017 年 9 月

原 子 核 物 理 评 论
Nuclear Physics Review

Vol. 34, No. 3
Sep., 2017

Article ID: 1007-4627(2017) 03-0563-06

Meson-meson Scattering in Hadronic Matter

XU Xiaoming

(*Department of Physics, Shanghai University, Shanghai 200444*)

Abstract: We have established a quark-interchange model and have proposed a quark-antiquark annihilation model to study meson-meson scattering. From QCD we obtain a temperature-dependent quark potential. The transition potential corresponding to quark-antiquark annihilation and creation is derived in perturbative QCD. The experimental ground-state meson masses are reproduced and the experimental data of elastic phase shifts for $\pi\pi$ scattering near the threshold energy in vacuum can be accounted for in the Born approximation. Starting from S-matrix element, we derive the transition amplitude and the cross section for the scattering. Unpolarised cross sections for reactions involving π, ρ, K and K* are calculated. Remarkable temperature dependence of the cross sections is found.

Key words: inelastic meson-meson scattering; quark interchange; quark-antiquark annihilation and creation

CLC number: O571.42 **Document code:** A **DOI:** 10.11804/NuclPhysRev.34.03.563

1 Introduction

Frequent scattering of mesons in hadroinc matter created in relativistic heavy-ion collisions significantly changes chemical equilibrium, hadron flow, hadron spectra and so on. All possible meson-meson scattering takes place in hadronic matter. The scattering is governed by resonance, quark interchange, quark-antiquark annihilation and creation. 2-to-2 meson-meson scattering in Fig. 1 is divided into four types. The first type involves quark interchange between scattering mesons. The second type involves quark-antiquark annihilation and creation. The third type involves both quark interchange and quark-antiquark annihilation and creation. The fourth type involves resonance and quark-antiquark annihilation and creation. In this talk I briefly summarize a study about the first, second and third types of scattering. Since pions, kaons and rho mesons are dominant meson species in hadronic matter, we focus on 2-to-2 scattering among π, ρ, K and K*. Much more details can be found in Refs. [1–4].

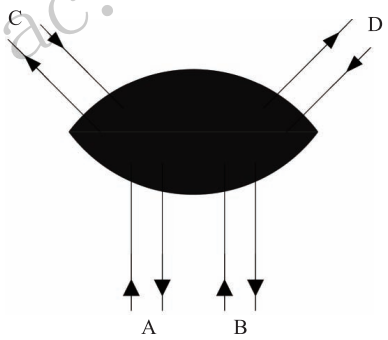

Fig. 1 Meson-meson scattering $\mathrm{A}+\mathrm{B}\to\mathrm{C}+\mathrm{D}$. Solid lines with up (down) triangles stand for quarks (antiquarks). The shaded area indicates resonance, quark interchange, quark-antiquark annihilation and creation.

2 Meson-meson scattering governed by quark interchange

Elastic meson-meson scattering such as $\pi\pi$ for $I=2$ and πK for $I=3/2$ has been studied in the quark interchange mechanism[5–8]. We study the following inelastic meson-meson scattering:

$$I=2\ \pi\pi\to\rho\rho,\quad I=1\ \mathrm{KK}\to\mathrm{K}^*\mathrm{K}^*,\quad I=1\ \mathrm{KK}^*\to\mathrm{K}^*\mathrm{K}^*,$$
$$I=\frac{3}{2}\ \pi K\to\rho K^*,\quad I=\frac{3}{2}\ \pi K^*\to\rho K^*,\quad I=\frac{3}{2}\ \rho K\to\rho K^*,\quad I=\frac{3}{2}\ \pi K^*\to\rho K.$$

Received date: 8 Dec. 2016; **Revised date:** 25 Apr. 2017

Foundation item: National Natural Science Foundation of China (11175111)

Biography: XU Xiaoming(1965–), male, Shaoxing, Zhejiang, Senior Scientist, Ph.D., working on nuclear physics;
E-mail: xmxu@staff.shu.edu.cn.

These reactions are represented by $A(q_1\bar{q}_1)+B(q_2\bar{q}_2) \to C(q_1\bar{q}_2)+D(q_2\bar{q}_1)$ which is caused by interchange of q_1 and q_2 or equivalently by interchange of $\bar{q}_1$ and $\bar{q}_2$. The S-matrix element for $A(q_1\bar{q}_1)+B(q_2\bar{q}_2) \to C(q_1\bar{q}_2)+D(q_2\bar{q}_1)$ is

$$S_{\rm fi}=\delta_{\rm fi}-2\pi i\delta(E_{\rm f}-E_{\rm i})<q_1\bar{q}_2,q_2\bar{q}_1|H_I|q_1\bar{q}_1,q_2\bar{q}_2>\ , \tag{1}$$

where $|q_1\bar{q}_1,q_2\bar{q}_2>$ ($|q_1\bar{q}_2,q_2\bar{q}_1>$) is the wave function of the initial (final) mesons; $E_{\rm i}$ ($E_{\rm f}$) is the total energy of the two initial (final) mesons. H_I is the sum of the interaction between one constiutent in meson A and one constituent in meson B for the scattering in the prior form,

$$H_I=V_{q_1\bar{q}_2}+V_{\bar{q}_1q_2}+V_{q_1q_2}+V_{\bar{q}_1\bar{q}_2}, \tag{2}$$

or H_I is the sum of the interaction between one constiutent in meson C and one constituent in meson D for the scattering in the post form,

$$H_I=V_{q_1\bar{q}_1}+V_{\bar{q}_2q_2}+V_{q_1q_2}+V_{\bar{q}_1\bar{q}_2}. \tag{3}$$

The interaction as a function of the distance $\boldsymbol{r}$ between two interacting constituents includes a spin-independent term denoted by $V_{\rm si}$ and a spin-spin interaction denoted by $V_{\rm ss}$,

$$V_{ab}=V_{\rm si}+V_{\rm ss}. \tag{4}$$

$V_{\rm si}$ depends on temperature T[9],

$$V_{\rm si}(\boldsymbol{r})=-\frac{\boldsymbol{\lambda}_a}{2}\cdot\frac{\boldsymbol{\lambda}_b}{2}\frac{3}{4}D\left[1.3-\left(\frac{T}{T_{\rm c}}\right)^4\right]\tanh(Ar)+\frac{\boldsymbol{\lambda}_a}{2}\cdot\frac{\boldsymbol{\lambda}_b}{2}\frac{6\pi}{25}\frac{v(\lambda r)}{r}\exp(-Er), \tag{5}$$

where $D=0.7$ GeV, $T_{\rm c}=0.175$ GeV, $A=1.5[0.75+0.25(T/T_{\rm c})^{10}]^6$ GeV, $E=0.6$ GeV and $\lambda=\sqrt{3b_0/16\pi^2\alpha'}$ in which $\alpha'=1.04$ GeV^{-2} and $b_0=11-\frac{2}{3}N_f$ with $N_f=4$. $\boldsymbol{\lambda}_a$ are the Gell-Mann matrices for the colour generators of constituent a. The dimensionless function $v(x)$ is given in Ref. [10]. $V_{\rm ss}$ is[11, 12]

$$V_{\rm ss}(\boldsymbol{r})=-\frac{\boldsymbol{\lambda}_a}{2}\cdot\frac{\boldsymbol{\lambda}_b}{2}\frac{16\pi^2}{25}\frac{d^3}{\pi^{3/2}}\exp(-{\rm d}^2r^2)\frac{\boldsymbol{s}_a\cdot\boldsymbol{s}_b}{m_am_b}+\frac{\boldsymbol{\lambda}_a}{2}\cdot\frac{\boldsymbol{\lambda}_b}{2}\frac{4\pi}{25}\frac{1}{r}\frac{{\rm d}^2v(\lambda r)}{{\rm d}r^2}\frac{\boldsymbol{s}_a\cdot\boldsymbol{s}_b}{m_am_b}, \tag{6}$$

where $\boldsymbol{s}_a$ and m_a are the spin and mass of constituent a, respectively, and d is related to quark masses. The short-distance part of $V_{\rm si}$ originates from one-gluon exchange plus one- and two-loop corrections. The intermediate- and long-distance part of $V_{\rm si}$ fits well the numerical potential obtained in the lattice gauge calculations[13]. The spin-spin interaction includes relativistic corrections to the gluon propagator.

It was shown in Ref. [11] that the spin-spin interaction in vacuum comes from the application of the Foldy-Wouthuysen canonical transformation to a relativistic two-particle Hamiltonian which contains the linear confinement and one-gluon exchange plus perturbative one- and two- loop corrections. The spin-spin interaction is related to the terms of the direct product of two Dirac α matrices in the Hamiltonian and the linear confinement in vacuum thus does not contribute to the spin-spin interaction. In this way the medium modification of the confinement also does not make a contribution to the spin-spin interaction and the spin-spin interaction in medium is the same as the spin-spin interaction in vacuum. In other words, the medium screening obtained in the lattice gauge calculations affects only the central spin-independent potential and the spin-spin interaction is temperature-independent.

The Schrödinger equation with V_{ab} at zero temperature is solved to reproduce the experimental masses of π, ρ, K, K*, J/ψ, ψ′, χ_c, D, D*, D_s and D_s^* mesons, while the masses of the up quark, the down quark, the strange quark and the charm quark are 0.32 GeV, 0.32 GeV, 0.5 GeV and 1.51 GeV, respectively. The Schrödinger equation with V_{ab} at nonzero temperatures provides meson masses at temperatures that are possessed by hadronic matter. As the temperature approaches the critical temperature, the π, ρ, K, and K* masses decrease rapidly and the spatial extension of the meson wave functions becomes wide rapidly. The π and ρ mesons (K and K*) become degenerate in mass at $T\to T_{\rm c}$.

The S-matrix element leads to the following transition amplitudes in momentum space[1],

$$\mathcal{M}_{\rm fi}^{\rm prior}=\sqrt{2E_{\rm A}2E_{\rm B}2E_{\rm C}2E_{\rm D}}\times\int\frac{{\rm d}^3p_{q_1\bar{q}_2}}{(2\pi)^3}\frac{{\rm d}^3p_{q_2\bar{q}_1}}{(2\pi)^3}\psi^+_{q_1\bar{q}_2}(\boldsymbol{p}_{q_1\bar{q}_2})\psi^+_{q_2\bar{q}_1}(\boldsymbol{p}_{q_2\bar{q}_1})\times(V_{q_1\bar{q}_2}+V_{\bar{q}_1q_2}+V_{q_1q_2}+V_{\bar{q}_1\bar{q}_2})\psi_{q_1\bar{q}_1}(\boldsymbol{p}_{q_1\bar{q}_1})\times\psi_{q_2\bar{q}_2}(\boldsymbol{p}_{q_2\bar{q}_2}), \tag{7}$$

for the prior form and

$$\mathcal{M}_{\rm fi}^{\rm post}=\sqrt{2E_{\rm A}2E_{\rm B}2E_{\rm C}2E_{\rm D}}\times\int\frac{{\rm d}^3p_{q_1\bar{q}_1}}{(2\pi)^3}\frac{{\rm d}^3p_{q_2\bar{q}_2}}{(2\pi)^3}\psi^+_{q_1\bar{q}_2}(\boldsymbol{p}_{q_1\bar{q}_2})\psi^+_{q_2\bar{q}_1}(\boldsymbol{p}_{q_2\bar{q}_1})\times(V_{q_1\bar{q}_1}+V_{\bar{q}_2q_2}+V_{q_1q_2}+V_{\bar{q}_1\bar{q}_2})\psi_{q_1\bar{q}_1}(\boldsymbol{p}_{q_1\bar{q}_1})\times\psi_{q_2\bar{q}_2}(\boldsymbol{p}_{q_2\bar{q}_2}), \tag{8}$$

for the post form. $E_{\rm A}$ ($E_{\rm B}$, $E_{\rm C}$, $E_{\rm D}$) is the energy of meson A (B, C, D); $\boldsymbol{p}_{ab}$ is the relative momentum of constituents a and b; the wave function ψ_{ab} stands for the product of colour, spin, flavour and quark-antiquark relative-motion wave functions of a and b. From the transition amplitudes the experimental data

of S-wave $I=2$ elastic phase shifts for $\pi\pi$ scattering in vacuum are reproduced.

The unpolarised cross section for the scattering in the prior form is

$$\sigma^{\rm prior}_{\rm unpol}(\sqrt{s},T)=\frac{1}{(2S_{\rm A}+1)(2S_{\rm B}+1)}\frac{1}{32\pi s}\frac{|\boldsymbol{P}'|}{|\boldsymbol{P}|}\times \sum_S(2S+1)\int_0^\pi {\rm d}\theta|\mathcal{M}^{\rm prior}_{\rm fi}(s,t)|^2\sin\theta, \quad (9)$$

where $\sqrt{s}$ is the total energy of the two initial mesons in the centre-of-mass frame; $S_{\rm A}$ and $S_{\rm B}$ are the spins of mesons A and B, respectively; S is the total spin of the two initial mesons; $\boldsymbol{P}$ and $\boldsymbol{P}'$ are the three-dimensional momenta of mesons A and C in the centre-of-mass frame, respectively; θ is the angle between $\boldsymbol{P}$ and $\boldsymbol{P}'$. The unpolarised cross section for the scattering in the post form is

$$\sigma^{\rm post}_{\rm unpol}(\sqrt{s},T)=\frac{1}{(2S_A+1)(2S_B+1)}\frac{1}{32\pi s}\frac{|\boldsymbol{P}'|}{|\boldsymbol{P}|}\times \sum_S(2S+1)\int_0^\pi {\rm d}\theta|\mathcal{M}^{\rm post}_{\rm fi}(s,t)|^2\sin\theta. \quad (10)$$

The unpolarised cross section for ${\rm A}({\rm q}_1\bar{\rm q}_1)+{\rm B}({\rm q}_2\bar{\rm q}_2)\to {\rm C}({\rm q}_1\bar{\rm q}_2)+{\rm D}({\rm q}_2\bar{\rm q}_1)$ is

$$\sigma^{\rm unpol}=\frac{1}{2}(\sigma^{\rm prior}_{\rm unpol}+\sigma^{\rm post}_{\rm unpol}). \quad (11)$$

Unpolarised cross sections for $\pi\pi\to\rho\rho$ for $I=2$, ${\rm KK}\to{\rm K^*K^*}$ for $I=1$, ${\rm KK^*}\to{\rm K^*K^*}$ for $I=1$, $\pi{\rm K}\to\rho{\rm K^*}$ for $I=\frac{3}{2}$, $\pi{\rm K^*}\to\rho{\rm K^*}$ for $I=\frac{3}{2}$, $\rho{\rm K}\to\rho{\rm K^*}$ for $I=\frac{3}{2}$ and $\pi{\rm K^*}\to\rho{\rm K}$ for $I=\frac{3}{2}$ have been shown in Figs. 2∼8 in Ref. [2] at the six temperatures $T/T_{\rm c}$=0, 0.65, 0.75, 0.85, 0.9 and 0.95. The 7 reactions are endothermic and their cross sections are 0 at threshold energies. The cross section for each reaction increases rapidly from 0 to a maximum and then decreases while $\sqrt{s}$ increases from the threshold energy. The peak cross section of each reaction changes considerably while temperature increases. It is due to the temperature dependence of the quark potential, meson masses and mesonic quark-antiquark relative-motion wave functions.

The peak cross sections of the 7 reactions have the same behavior: each decreases from $T/T_{\rm c}=0$ to a value and increases from the value to 0.95. As the temperature increases from zero, the long-distance part of the potential gradually becomes a distance-independent and temperature-dependent value, confinement becomes weaker and weaker, the Schrödinger equation produces increasing meson radii, and mesonic bound states become looser and looser. The weakening confinement with increasing temperature makes combining final quarks and antiquarks into mesons more difficult and thus reduces the cross sections. From $T/T_{\rm c}=0$ to the value the peak cross section, which increases with slowly increasing radii of the initial mesons, cannot balance the decrease in the cross sections due to the weakening confinement; thus, the peak cross sections decrease. From the value to 0.95 the peak cross section, which is increased by the rapidly increasing radii of the initial mesons, overcomes the decrease in the cross sections by the weakening confinement; thus, the peak cross sections increase.

3 Meson-meson scattering governed by quark-antiquark annihilation and creation

We study the following reactions:

$$\begin{aligned}&I=1\ \pi\pi\to\rho\rho,\ {\rm K\bar K}\to{\rm K^*\bar K^*},\ {\rm K\bar K^*}\to{\rm K^*\bar K^*},\\ &\quad {\rm K^*\bar K}\to{\rm K^*\bar K^*},\\ &I=1\ \pi\pi\to{\rm K\bar K},\ \pi\rho\to{\rm K\bar K^*},\ \pi\rho\to{\rm K^*\bar K},\ {\rm K\bar K}\to\rho\rho.\end{aligned}$$

These reactions are represented by ${\rm A}({\rm q}_1\bar{\rm q}_1)+{\rm B}({\rm q}_2\bar{\rm q}_2)\to{\rm C}({\rm q}_3\bar{\rm q}_1)+{\rm D}({\rm q}_2\bar{\rm q}_4)$ due to ${\rm q}_1+\bar{\rm q}_2\to{\rm q}_3+\bar{\rm q}_4$ or ${\rm A}({\rm q}_1\bar{\rm q}_1)+{\rm B}({\rm q}_2\bar{\rm q}_2)\to{\rm C}({\rm q}_1\bar{\rm q}_4)+{\rm D}({\rm q}_3\bar{\rm q}_2)$ due to $\bar{\rm q}_1+{\rm q}_2\to{\rm q}_3+\bar{\rm q}_4$. The S-matrix element for ${\rm A+B\to C+D}$ is

$$\begin{aligned}S_{\rm fi}=&\delta_{\rm fi}-2\pi i\delta(E_{\rm f}-E_{\rm i})\times\\ &(<{\rm q}_3\bar{\rm q}_1,{\rm q}_2\bar{\rm q}_4\,|\,V_{{\rm aq}_1\bar{\rm q}_2}\,|\,{\rm q}_1\bar{\rm q}_1,{\rm q}_2\bar{\rm q}_2>+\\ &<{\rm q}_1\bar{\rm q}_4,{\rm q}_3\bar{\rm q}_2\,|\,V_{{\rm a}\bar{\rm q}_1{\rm q}_2}\,|\,{\rm q}_1\bar{\rm q}_1,{\rm q}_2\bar{\rm q}_2>)\ , \end{aligned}\quad (12)$$

where $|{\rm q}_3\bar{\rm q}_1,{\rm q}_2\bar{\rm q}_4>$ and $|{\rm q}_1\bar{\rm q}_4,{\rm q}_3\bar{\rm q}_2>$ are the wave functions of the final mesons; $V_{{\rm aq}_1\bar{\rm q}_2}$ and $V_{{\rm a}\bar{\rm q}_1{\rm q}_2}$ are the transition potentials for the processes ${\rm q}_1+\bar{\rm q}_2\to{\rm q}_3+\bar{\rm q}_4$ and $\bar{\rm q}_1+{\rm q}_2\to{\rm q}_3+\bar{\rm q}_4$, respectively. The S-matrix element leads to the following transition amplitudes[3],

$$\begin{aligned}\mathcal{M}_{{\rm aq}_1\bar{\rm q}_2}=&\sqrt{2E_{\rm A}2E_{\rm B}2E_{\rm C}2E_{\rm D}}\int\frac{{\rm d}^3p_{{\rm q}_1\bar{\rm q}_1}}{(2\pi)^3}\frac{d^3p_{{\rm q}_2\bar{\rm q}_2}}{(2\pi)^3}\times\\ &\psi^+_{{\rm q}_3\bar{\rm q}_1}(\boldsymbol{p}_{{\rm q}_3\bar{\rm q}_1})\psi^+_{{\rm q}_2\bar{\rm q}_4}(\boldsymbol{p}_{{\rm q}_2\bar{\rm q}_4})V_{{\rm aq}_1\bar{\rm q}_2}(\boldsymbol{k})\times\\ &\psi_{{\rm q}_1\bar{\rm q}_1}(\boldsymbol{p}_{{\rm q}_1\bar{\rm q}_1})\psi_{{\rm q}_2\bar{\rm q}_2}(\boldsymbol{p}_{{\rm q}_2\bar{\rm q}_2}),\end{aligned}\quad (13)$$

corresponding to ${\rm q}_1+\bar{\rm q}_2\to{\rm q}_3+\bar{\rm q}_4$ and

$$\begin{aligned}\mathcal{M}_{{\rm a}\bar{\rm q}_1{\rm q}_2}=&\sqrt{2E_{\rm A}2E_{\rm B}2E_{\rm C}2E_{\rm D}}\int\frac{{\rm d}^3p_{{\rm q}_1\bar{\rm q}_1}}{(2\pi)^3}\frac{{\rm d}^3p_{q_2\bar{\rm q}_2}}{(2\pi)^3}\times\\ &\psi^+_{{\rm q}_1\bar{\rm q}_4}(\boldsymbol{p}_{{\rm q}_1\bar{\rm q}_4})\psi^+_{{\rm q}_3\bar{\rm q}_2}(\boldsymbol{p}_{{\rm q}_3\bar{\rm q}_2})V_{{\rm a}\bar{\rm q}_1{\rm q}_2}(\boldsymbol{k})\times\\ &\psi_{{\rm q}_1\bar{\rm q}_1}(\boldsymbol{p}_{{\rm q}_1\bar{\rm q}_1})\psi_{{\rm q}_2\bar{\rm q}_2}(\boldsymbol{p}_{{\rm q}_2\bar{\rm q}_2}),\end{aligned}\quad (14)$$

corresponding to $\bar{\rm q}_1+{\rm q}_2\to{\rm q}_3+\bar{\rm q}_4$.

A quark with momentum p_1 and an antiquark with momentum $-p_2$ annihilate into a gluon with momentum k, and subsequently this gluon creates a quark with momentum p_3 and an antiquark with momentum $-p_4$. Within perturbative QCD we obtain the transition potential for ${\rm q}({\rm p}_1)+\bar{\rm q}(-{\rm p}_2)\to{\rm q}'({\rm p}_3)+\bar{\rm q}'(-{\rm p}_4)$ in

momentum space,

$$V_{\mathrm{aq\bar{q}}}(\boldsymbol{k})=\frac{g_{\mathrm{s}}^2}{k^2}\frac{\boldsymbol{\lambda}(34)}{2}\cdot\frac{\boldsymbol{\lambda}(21)}{2}\Big(\frac{\boldsymbol{\sigma}(34)\cdot\boldsymbol{k}\boldsymbol{\sigma}(21)\cdot\boldsymbol{k}}{4m_{q'}m_q}-\boldsymbol{\sigma}(34)\cdot\boldsymbol{\sigma}(21)-\frac{\boldsymbol{\sigma}(21)\cdot\boldsymbol{p}_2\boldsymbol{\sigma}(34)\cdot\boldsymbol{\sigma}(21)\boldsymbol{\sigma}(21)\cdot\boldsymbol{p}_1}{4m_q^2}-\frac{\boldsymbol{\sigma}(34)\cdot\boldsymbol{p}_3\boldsymbol{\sigma}(34)\cdot\boldsymbol{\sigma}(21)\boldsymbol{\sigma}(34)\cdot\boldsymbol{p}_4}{4m_{q'}^2}\Big),\quad(15)$$

where g_{s} is the gauge coupling constant; m_q ($m_{q'}$) is the q (q') mass; $\boldsymbol{\lambda}(ij)$ ($\boldsymbol{\sigma}(ij)$) mean that they have matrix elements between the colour (spin) wave functions of constituents i and j.

Confinement is a result of multi-gluon exchange between two constituents. The medium modification of the confinement gives rise to the temperature dependence of the quark potential which is used in Eqs. (2) and (3). The transition potential given in Eq. (15) corresponds to only one gluon. Therefore, the transition potential is temperature-independent.

Including colour, spin and flavour matrix elements, the transition amplitudes are given upon integrating over the relative momenta of the quark and the antiquark of the two initial mesons. With the transition amplitudes the experimental data of S-wave $I=0$ and P-wave $I=1$ elastic phase shifts for $\pi\pi$ scattering near the threshold energy are reproduced.

The unpolarised cross section for A+B → C+D via quark-antiquark annihilaiton and creation is

$$\sigma^{\mathrm{unpol}}(\sqrt{s},T)=\frac{1}{(2J_{\mathrm{A}}+1)(2J_{\mathrm{B}}+1)}\frac{1}{32\pi s}\frac{|\boldsymbol{P}'|}{|\boldsymbol{P}|}\int_0^{\pi}\mathrm{d}\theta\sum_{J_{\mathrm{A}z}J_{\mathrm{B}z}J_{\mathrm{C}z}J_{\mathrm{D}z}}|\mathcal{M}_{\mathrm{aq_1\bar{q}_2}}+\mathcal{M}_{\mathrm{a\bar{q}_1q_2}}|^2\sin\theta,\quad(16)$$

where $J_{\mathrm{A}z}$ ($J_{\mathrm{B}z}$, $J_{\mathrm{C}z}$, $J_{\mathrm{D}z}$) is the magnetic projection quantum number of the angular momentum J_{A} (J_{B}, J_{C}, J_{D}) of meson A (B, C, D). In Figs. 7∼15 in Ref. [3] we have shown unpolarised cross sections for the nine channels:

$$\begin{aligned}
&I=1\ \pi\pi\to\rho\rho,\ I=1\ \mathrm{K\bar{K}}\to\mathrm{K^*\bar{K}^*},\\
&\qquad\qquad I=0\ \mathrm{K\bar{K}}\to\mathrm{K^*\bar{K}^*},\\
&I=1\ \mathrm{K\bar{K}^*}\to\mathrm{K^*\bar{K}^*},\ I=0\ \mathrm{K\bar{K}^*}\to\mathrm{K^*\bar{K}^*},\\
&\qquad\qquad I=1\ \pi\pi\to\mathrm{K\bar{K}},\\
&I=1\ \pi\rho\to\mathrm{K\bar{K}^*},\ I=1\ \pi\mathrm{\rho}\to\mathrm{K^*\bar{K}},\ I=1\ \mathrm{K\bar{K}}\to\rho\rho.
\end{aligned}$$

All the channels except $\mathrm{K\bar{K}}\to\rho\rho$ for $I=1$ are endothermic. In vacuum the ρ mass is larger than the kaon mass. When the temperature increases, the ρ mass decreases faster than the kaon mass. At $T=0.785T_{\mathrm{c}}$ the ρ mass equals the kaon mass. Below $T=0.785T_{\mathrm{c}}$ the reaction $\mathrm{K\bar{K}}\to\rho\rho$ for $I=1$ is endothermic because the sum of the two ρ masses is larger than the sum of the kaon and antikaon masses; otherwise, it is exothermic. In contrast to any endothermic reaction which has the zero cross section at the threshold due to $\boldsymbol{P}'=0$, the exothermic reaction has the infinite cross section at the threshold due to $\boldsymbol{P}=0$. When $\sqrt{s}$ increases from the threshold energies, the cross sections for the exothermic reactions decrease very rapidly from infinity.

The peak cross section of each channel varies rapidly with increasing temperature. It is due to differences among mesonic temperature dependence in hadronic matter. When $\sqrt{s}$ increases from the magnitude that corresponds to the peak cross section, the cross section for $\pi\pi\to\rho\rho$ for $I=1$, $\mathrm{K\bar{K}^*}\to\mathrm{K^*\bar{K}^*}$ for $I=1$ or $\pi\rho\to\mathrm{K^*\bar{K}}$ for $I=1$ decreases slowly. This behaviour quite differs from that for the reaction which is governed by the quark interchange.

4 Meson-meson scattering governed by quark interchange as well as quark-antiquark annihilation and creation

Meson-meson reactions may involve not only quark interchange but also quark-antiquark annihilation and creation. We study this type of scattering with

$$I=0\ \pi\pi\to\rho\rho,\ I=\frac{1}{2}\ \pi\mathrm{K}\to\rho\mathrm{K^*},\ I=\frac{1}{2}\ \pi\mathrm{K^*}\to\rho\mathrm{K},$$
$$I=\frac{1}{2}\ \pi\mathrm{K^*}\to\rho\mathrm{K^*},\ I=\frac{1}{2}\ \rho\mathrm{K}\to\rho\mathrm{K^*}.$$

These reactions are represented by $\mathrm{A(q_1\bar{q}_1)+B(q_2\bar{q}_2)}\to\mathrm{C(q_1\bar{q}_2}$ or $\mathrm{q_3\bar{q}_1}$ or $\mathrm{q_1\bar{q}_4)+D(q_2\bar{q}_1}$ or $\mathrm{q_2\bar{q}_4}$ or $\mathrm{q_3\bar{q}_2)}$. Meson C (D) has the constituents $\mathrm{q_1\bar{q}_2}$, $\mathrm{q_3\bar{q}_1}$ or $\mathrm{q_1\bar{q}_4}$ ($\mathrm{q_2\bar{q}_1}$, $\mathrm{q_2\bar{q}_4}$ or $\mathrm{q_3\bar{q}_2}$) depending on the processes embedded in the reactions. The S-matrix element for $\mathrm{A+B\to C+D}$ is

$$\begin{aligned}
S_{\mathrm{fi}}=&\delta_{\mathrm{fi}}-2\pi i\delta(E_{\mathrm{f}}-E_{\mathrm{i}})(<\mathrm{q_1\bar{q}_2,q_2\bar{q}_1}|H_{\mathrm{I}}|\mathrm{q_1\bar{q}_1,q_2\bar{q}_2}>+\\
&<\mathrm{q_3\bar{q}_1,q_2\bar{q}_4}|V_{\mathrm{aq_1\bar{q}_2}}|\mathrm{q_1\bar{q}_1,q_2\bar{q}_2}>+\\
&<\mathrm{q_1\bar{q}_4,q_3\bar{q}_2}|V_{\mathrm{a\bar{q}_1q_2}}|\mathrm{q_1\bar{q}_1,q_2\bar{q}_2}>).
\end{aligned}\quad(17)$$

From the S-matrix element the transition amplitude is

$$\mathcal{M}_{\mathrm{fi}}^{\mathrm{pr}}=\mathcal{M}_{\mathrm{fi}}^{\mathrm{prior}}+\mathcal{M}_{\mathrm{aq_1\bar{q}_2}}+\mathcal{M}_{\mathrm{a\bar{q}_1q_2}},\quad(18)$$

for the reaction including the quark-interchange process in the prior form or

$$\mathcal{M}_{\mathrm{fi}}^{\mathrm{pt}}=\mathcal{M}_{\mathrm{fi}}^{\mathrm{post}}+\mathcal{M}_{\mathrm{aq_1\bar{q}_2}}+\mathcal{M}_{\mathrm{a\bar{q}_1q_2}},\quad(19)$$

for the reaction including the quark-interchange process in the post form. Corresponding to $\mathcal{M}_{\mathrm{fi}}^{\mathrm{pr}}$ and $\mathcal{M}_{\mathrm{fi}}^{\mathrm{pt}}$ we have

$$\sigma_{\mathrm{unpol}}^{\mathrm{prior}}(\sqrt{s},T)=\frac{1}{(2J_{\mathrm{A}}+1)(2J_{\mathrm{B}}+1)}\frac{1}{32\pi s}\frac{|\boldsymbol{P}'|}{|\boldsymbol{P}|}\times\int_0^{\pi}\mathrm{d}\theta\sum_{J_{\mathrm{A}z}J_{\mathrm{B}z}J_{\mathrm{C}z}J_{\mathrm{D}z}}|\mathcal{M}_{\mathrm{fi}}^{\mathrm{pr}}|^2\sin\theta,\quad(20)$$

$$\sigma^{\rm post}_{\rm unpol}(\sqrt{s},T)=\frac{1}{(2J_{\rm A}+1)(2J_{\rm B}+1)}\frac{1}{32\pi s}\frac{|\boldsymbol{P}'|}{|\boldsymbol{P}|}\times \int_0^{\pi}{\rm d}\theta\sum_{J_{\rm Az}J_{\rm Bz}J_{\rm Cz}J_{\rm Dz}}|\mathcal{M}^{\rm pt}_{\rm fi}|^2\sin\theta. \quad (21)$$

The unpolarised cross section for $\rm A+B\to C+D$ is

$$\sigma^{\rm unpol}(\sqrt{s},T)=\frac{1}{2}\left[\sigma^{\rm prior}_{\rm unpol}(\sqrt{s},T)+\sigma^{\rm post}_{\rm unpol}(\sqrt{s},T)\right]. \quad (22)$$

The cross section for $\pi\pi\to\rho\rho$ for $I=0$ is shown in Fig. 16 in Ref. [3]. The cross sections for $\pi{\rm K}^*\to\rho{\rm K}$ for $I=1/2$, $\pi{\rm K}^*\to\rho{\rm K}^*$ for $I=1/2$, $\pi{\rm K}\to\rho{\rm K}^*$ for $I=1/2$ and $\rho{\rm K}\to\rho{\rm K}^*$ for $I=1/2$ are shown in Figs. 3∼6 in Ref. [4]. Quark interchange plays a role mainly near the threshold and even dominates the reactions near the critical temperature. When $\sqrt{s}$ is far away from the threshold, the contribution of quark-antiquark annihilation and creation to the cross sections is so obvious that a wide peak may appear in a temperature region.

5 Parametrizations of numerical cross sections

Starting from an effective Lagrangian, cross sections for $\pi\pi\to{\rm K}\bar{\rm K}$, $\rho\rho\to{\rm K}\bar{\rm K}$, $\pi\rho\to{\rm K}\bar{\rm K}^*$ and $\pi\rho\to{\rm K}^*\bar{\rm K}$ through one-meson exchange in vacuum have been obtained in Ref. [14]. The cross sections for the four reactions have been used to describe the evolution of hadronic matter created in relativistic heavy-ion collisions. In the present work we have obtained cross sections for more than the four reactions. But the cross sections are numerical. To use our cross sections conveniently in the evolution of hadronic matter, we parametrize the numerical cross sections. The parametrizations are

$$\sigma^{\rm unpol}(\sqrt{s},T)= a_1\left(\frac{\sqrt{s}-\sqrt{s_0}}{b_1}\right)^{c_1}\exp\left[c_1\left(1-\frac{\sqrt{s}-\sqrt{s_0}}{b_1}\right)\right]+ a_2\left(\frac{\sqrt{s}-\sqrt{s_0}}{b_2}\right)^{c_2}\exp\left[c_2\left(1-\frac{\sqrt{s}-\sqrt{s_0}}{b_2}\right)\right], \quad (23)$$

for the endothermic reactions and

$$\sigma^{\rm unpol}(\sqrt{s},T)= \frac{\boldsymbol{P}'^2}{\boldsymbol{P}^2}\left\{a_1\left(\frac{\sqrt{s}-\sqrt{s_0}}{b_1}\right)^{c_1}\exp\left[c_1\left(1-\frac{\sqrt{s}-\sqrt{s_0}}{b_1}\right)\right]+ a_2\left(\frac{\sqrt{s}-\sqrt{s_0}}{b_2}\right)^{c_2}\exp\left[c_2\left(1-\frac{\sqrt{s}-\sqrt{s_0}}{b_2}\right)\right]\right\}, \quad (24)$$

for the exothermic reactions. $\sqrt{s_0}$ is the threshold energy. The parameters a_1, b_1, c_1, a_2, b_2 and c_2 are listed in Tables 1 and 2 in Ref. [2], in Tables 2∼4 in Ref. [3] and in Table 2 in Ref. [4].

6 Conclusions

We have established a quark-interchange model to study meson-meson scattering. A temperature-dependent quark potential is given to yield meson masses and mesonic quark-antiquark wave functions. The transition amplitudes for the prior form and the post form are derived from the S-matrix element and are used to calculate the elastic phase shifts for $\pi\pi$ scattering and the unpolarised cross sections for the first type of inelastic meson-meson scattering.

We have proposed a model with quark-antiquark annihilation and creation to study meson-meson scattering. The transition potential for quark-antiquark annihilation and creation is derived in perturbative QCD. The transition potential and the transition amplitudes derived from the S-matrix element are used to calculate the elastic phase shifts for $\pi\pi$ scattering and the unpolarised cross sections for the second type of inelastic meson-meson scattering.

Combining the quark-interchange model and the quark-antiquark annihilation model, we have studied the meson-meson scattering that is governed by quark interchange as well as quark-antiquark annihilation and creation. The relevant transition amplitude is the sum of the one corresponding to quark interchange and the one corresponding to quark-antiquark annihilation and creation. With the transition amplitude we obtain the unpolarised cross sections for the third type of inelastic meson-meson scattering.

Depending on temperature, a reaction is either endothermic or exothermic. The cross sections for the reactions governed by quark-antiquark annihilation and creation are quite different from the cross sections for the reactions governed by quark interchange. While quark interchange plays a role mainly near the threshold energy, quark-antiquark annihilation and creation does in a wide regime of energy. Remarkable temperature dependence of the unpolarised cross sections is found.

References:

[1] LI Y Q, XU X M. Nucl Phys A, 2007, **794**: 210.
[2] SHEN Z Y, XU X M. J Korean Phys Soc, 2015, **66**: 754.
[3] SHEN Z Y, XU X M, WEBER H J. Phys Rev D, 2016, **94**: 034030.
[4] YANG K, XU X M, WEBER H J. arXiv:1708.03062.
[5] BARNES T, SWANSON E S. Phys Rev D, 1992, **46**: 131.
[6] SWANSON E S. Ann Phys (N Y), 1992, **220**: 73.
[7] BARNES T, SWANSON E S, WEINSTEIN J. Phys Rev D, 1992, **46**: 4868.
[8] BARNES T, BLACK N, SWANSON E S. Phys Rev C, 2001, **63**: 025204.
[9] ZHANG Y P, XU X M, GE H J. Nucl Phys A, 2010, **832**: 112.

[10] BUCHMÜLLER W, TYE S H H. Phys Rev D, 1981, **24**: 132.
[11] XU X M. Nucl Phys A, 2002, **697**: 825.
[12] ZHOU J, XU X M. Phys Rev C, 2012, **85**: 064904.
[13] KARSCH F, LAERMANN E, PEIKERT A. Nucl Phys B, 2001, **605**: 579.
[14] BROWN G E, KO C M, WU Z G, *et al*. Phys Rev C, 1991, **43**: 1881.

强子物质中的介子-介子散射

许晓明[1)]

(上海大学物理系，上海 200444)

摘要： 建立了一个夸克交换模型和提出了一个夸克-反夸克湮灭模型来研究介子-介子散射。从量子色动力学我们得到一个依赖于温度的夸克作用势。从微扰量子色动力学推导对应于夸克-反夸克湮灭和产生的跃迁势。模型给出基态介子质量的实验值，并且在玻恩近似下能说明真空中阈能附近的π-π弹性散射相移的实验值。从S矩阵元出发，推导散射的跃迁振幅和截面公式。计算出涉及π, ρ, K, K*的反应的非极化截面。发现这些截面具有强烈的温度依赖性。

关键词： 非弹性介子-介子散射；夸克交换；夸克-反夸克湮灭和产生

收稿日期： 2016-12-08； **修改日期：** 2017-04-25
基金项目： 国家自然科学基金资助项目(11175111)
1) E-mail: xmxu@staff.shu.edu.cn。